Synthesis and evaluation of radioiodinated 1-{2-[5-(2-methoxyethoxy)-1*H*-benzo[*d*]imidazol-1-yl]quinolin-8-yl}piperidin-4-amine derivatives for platelet-derived growth factor receptor β (PDGFRβ) imaging

Abstract

Platelet-derived growth factor receptor β (PDGFRβ) is a transmembrane tyrosine kinase receptor and it is upregulated in various malignant tumors. Radiolabeled PDGFRβ inhibitors can be a convenient tool for the imaging of tumors overexpressing PDGFRβ. In this study, [^{125}I]-1-{5-iodo-2-[5-(2-methoxyethoxy)-1*H*-benzo[*d*]imidazol-1-yl)quinoline-8-yl}piperidin-4-amine ([^{125}I]IIQP) and [^{125}I]-*N*-3-iodobenzoyl-1-{2-[5-(2-methoxyethoxy)-1*H*-benzo[*d*]imidazol-1-yl]quinolin-8-yl}-piperidin-4-amine ([^{125}I]IB-IQP) were designed and synthesized, and their potential as PDGFRβ imaging agents was evaluated. In cellular uptake experiments, [^{125}I]IIQP and [^{125}I]IB-IQP showed higher uptake by PDGFRβ-positive cells than by PDGFRβ-negative cells, and the uptake in PDGFRβ-positive cells was inhibited by co-culture with PDGFRβ ligands. The biodistribution of both radiotracers in normal mice exhibited hepatobiliary excretion as the main route. In mice inoculated with BxPC3-luc (PDGFRβ-positive), the tumor uptake of radioactivity at 1 h after the injection of [^{125}I]IIQP was significantly higher than that after the injection of [^{125}I]IB-IQP. These results indicated that [^{125}I]IIQP can be a suitable PDGFRβ imaging agent. However, further modification of its structure will be required to obtain a more appropriate PDGFRβ-targeted imaging agent with a higher signal / noise ratio.

Keywords: radiotracer, molecular imaging, PDGFRβ, tyrosine kinase inhibitor

1. Introduction

PDGFRβ belongs to a subfamily of receptor tyrosine kinases (RTKs). It possesses an outer membrane with a PDGF ligand binding site and an inner membrane tyrosine kinase (TK) domain with an adenosine three phosphate (ATP) binding site.[1] Binding of PDGF ligands to the extracellular binding domain triggers PDGFRβ dimerization, thus inducing phosphorylation of its intracellular regions due to an activated ATP-binding domain. This is followed by the activation of signaling pathways that regulate important cellular functions.[2] The expression of PDGFRβ is highly restricted in most normal cells; however, upregulation of PDGFRβ in numerous human tumors and its relationship with tumor progression features such as cell migration, metastasis, angiogenesis, and proliferation, have been reported.[3-5] Therefore, PDGFRβ can be an attarctive target not only for cancer therapy but also for developing tumor-imaging agents.[6-8]

Nuclear medicine has been a revolutionary invention in the field of diagnostic imaging because it is noninvasive and facilitates continous monitoring of disease progression or treatment response.[9,10] Moreover, the imaging modalities in nuclear medicine, such as single photon emission computed tomography (SPECT) and positron emission tomography (PET) can quantify receptor density and molecular target expression in patients, thus becoming a useful tool in drug development.[10-12] Previous studies have reported imaging agents, including radiolabeled protein,[13,14] aptamer,[15] affibody molecules,[16,17] and peptide[18,19] that target the extracellular parts of PDGFRβ. Although the imaging of intracellular parts of PDGFRβ, particularly its ATP-binding site, has hardly been reported,[8] the ATP-binding is very important for following signal transductions and growth of cancer cells. Therefore, the ATP-binding site can be a target for TK inhibitors (TKIs). Meanwhile, mutations of the ATP-binding site have frequently been found[20,21]. The mutation status often affects therapeutic effects of TKIs. Thus, the information of the ATP-binding site, containing the mutation status, is useful for the prediction of therapeutic effects of TKIs. Other radiolabeled TK inhibitors (TKIs)[22-26] and their potential advantages, such as assessment of drug sensitivity[20], mutation status[21], and usefulness in drug screening[11,27,28] have been demonstrated.

1-{2-[5-(2-Methoxyethoxy)-1*H*-benzo[*d*]imidazol-1-yl]quinolin-8-yl}piperidin-4-amine (CP-673451, IQP) (Figure 1) is a highly selective benzimidazole inhibitor of PDGFRβ (IC_{50} = 1 nM) over PDGFRα (IC_{50} = 10 nM). Importantly, it is 1,000 times selective compared with many other RTKs. It competitively inhibits ATP-binding to the ATP-binding site of PDGFRβ and blocks phosphorylation.[29,30] High binding affinity and high selectivity to the molecular target are important for a lead compound of imaging probes. IQP can be an attractive compound in an attempt to image the ATP binding site of PDGFRβ. Therefore, we speculated that radiolabeled IQP derivatives that bind the ATP-binding site may be useful imaging probes.

To develop novel radiolabeled molecular probes for PDGFRβ imaging, we chose radioiodine as a radionuclide in this study because ^{123}I ($t_{1/2}$ = 13.2 h) and ^{124}I ($t_{1/2}$ = 4.2 d) are useful radionuclides for SPECT and PET, respectively. We did not have sufficient information about the introduction of radioiodine into IQP structure to retain high affinity for PDGFRβ. To evaluate the feasibility of IQP derivatives as PDGFRβ imaging probes, we designed and synthesized two different types of iodine labeled IQP, 1-{5-iodo-2-[5-(2-methoxyethoxy)-1*H*-benzo[*d*]imidazol-1-yl]quinolin-8-yl}piperidin-4-amine (IIQP) and *N*-3-iodobenzoyl-1-{2-[5-(2-methoxyethoxy)-1*H*-benzo[*d*]imidazol-1-yl]-quinolin-8-yl}-piperidin-4-amine (IB-IQP). In IIQP, iodine was directly introduced to C-5 of the quinoline group of IQP because it is a reactive site for halogenation of IQP. In IB-IQP, iodine was indirectly introduced by conjugation of 3-iodo benzoyl group using SIB (*N*-succinimidyl-3-iodobenzoate) with the primary amine group of IQP. We then examined the binding affinities of two derivatives for PDGFRβs. Subsequently, radiotracers [^{125}I]IIQP and [^{125}I]IB-IQP (Figure 1) were synthesized and evaluated *in vitro* and *in vivo* to investigate their usefulness as PDGFRβ imaging agents. Although we are interested in developing imaging probes for SPECT and PET, ^{125}I was used as an alternative radionuclide in these initial studies because of its long half-life ($t_{1/2}$ = 59.4 d).

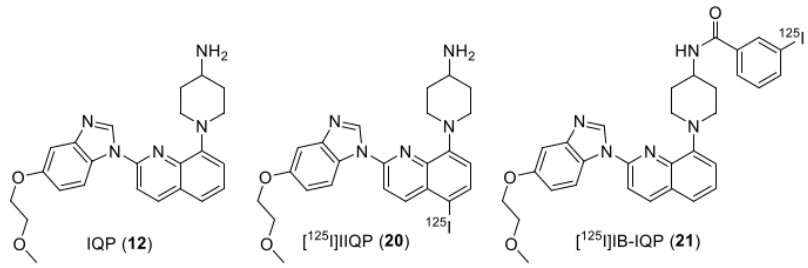

Figure 1. Chemical structures of IQP, [^{125}I]IIQP, and [^{125}I]IB-IQP.

2. Results

2.1. Synthesis of reference compounds and precursors

Lead compound **12** (Scheme 1) and the non-radioactive iodinated reference compounds, **13** and **18,** were easily obtained. Iodine was incorporated to the C-5 of quinoline core of IQP using mixture reagents of NCS and NaI with stirring at 50 °C for 18 h in acetic acid to obtain compound **13** (Scheme 2). On the other hand, compound **18** was synthesized by stirring the mixture of synthesized SIB and IQP at 50 °C for 2 h in a basic solution (Scheme 3). Retention time for compounds **13** and **18** on RP-HPLC were 11.7 and 12.5 min, respectively (Supporting Information). For synthesis of tin precursor **15**, utilizing the Pd(0) catalyst, tri-butyl tin group was introduced into IQP instead of iodine in **14** to obtain compound **15** in 48% yield after purification using RP-HPLC. Meanwhile, compound **19** was obtained by the reaction between ATE and IQP with 56% yield.

2.2. Cell viability assays

To assess the binding potential of IIQP and IB-IQP to the ATP-binding site of PDGFRβ, TR-PCT1 cells were cultured in the presence of various concentration of IQP, IIQP, or IB-IQP (1 – 1000 nM). As displayed in Figure 2, the effects of IB-IQP were similar to those of IQP; however, IIQP was more effective than IQP in reducing the viability of TR-PCT1 cells.

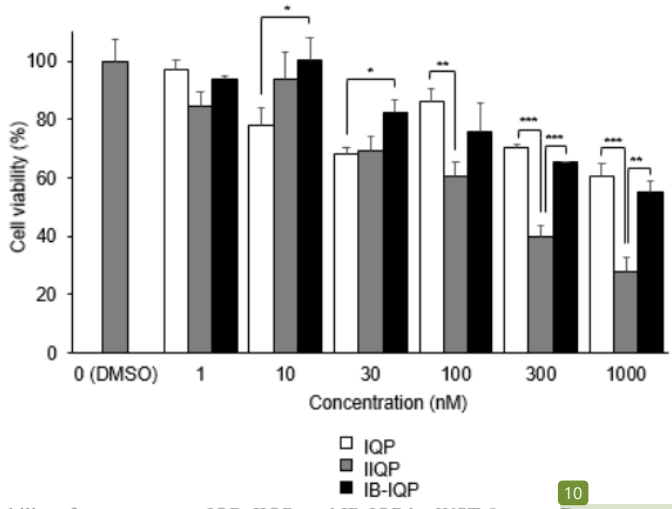

Figure 2. Cell viability after exposure to IQP, IIQP, and IB-IQP by WST-8 assay. Data are presented as mean ± SD for three samples. Significance was determined using a one-way ANOVA followed by Tukey's post hoc test ($^{*}p < 0.05$, $^{**}p < 0.01$, $^{***}p < 0.001$).

2.3. Radiolabeling

Two novel ^{125}I labeled IQP, [^{125}I]IIQP and [^{125}I]IB-IQP, were synthesized by an iododestannylation reaction with the corresponding tributyltin precursors, as outlined in Schemes 2 and 3, respectively. Both these radiotracers were synthesized using NCS as an oxidizing agent in an

acidic solution at room temperature in high radiochemical yield (95 and 85%, respectively). After purification using RP-HPLC, the radiochemical purities were over 99%.

2.4. Partition coefficient

The *n*-octanol/PB partition coefficients for [^{125}I]IIQP and [^{125}I]IB-IQP were 2.71 ± 0.03 and 3.19 ± 0.17, respectively. Lipophilicity of [^{125}I]IB-IQP was higher than that of [^{125}I]IIQP.

2.5. In vitro stability assay

The stability of radiotracers in 0.1 M PBS (pH 7.4) was evaluated using TLC analysis and confirmed using HPLC. After incubation for 24 h at 37 °C, the purity of the radiotracers remained high, and 93.9 ± 0.4% of [^{125}I]IIQP and 94.1 ± 0.7% of [^{125}I]IB-IQP remained intact.

2.6. Cell uptake study

The *in vitro* cell uptake experiments of [^{125}I]IIQP and [^{125}I]IB-IQP were performed using two types of cell lines: PDGFRβ-positive BxPC3-luc cells and PDGFRβ-negative MCF7 cells.[15,18,40] As shown in Figure 3, BxPC3-luc cells showed higher uptake of [^{125}I]IIQP and [^{125}I]IB-IQP then that by MCF7 cells. The uptake of [^{125}I]IIQP in BxPC3-luc cells reached 2.34 %dose/μg protein after 4 h incubation, whereas that of [^{125}I]IB-IQP reached 0.95 %dose/μg protein.

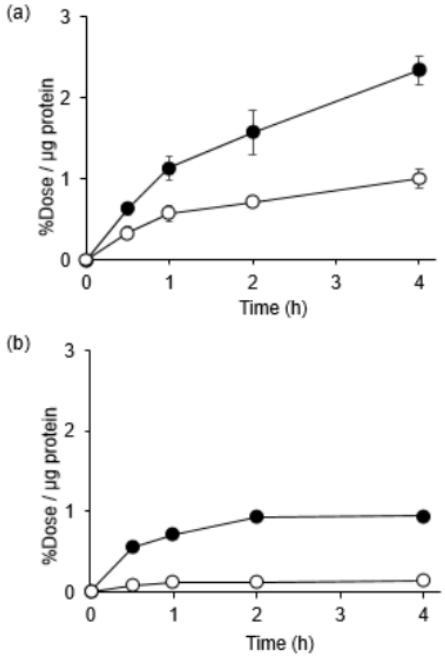

Figure 3. Cellular uptake study. Time-dependent accumulation of (a) [^{125}I]IIQP and (b) [^{125}I]IB-IQP in BxPC3-luc (closed circles) and MCF7 (open circles) cells. Data were presented as mean ± SD for three samples.

In the blocking studies, the uptakes of [^{125}I]IIQP and [^{125}I]IB-IQP in BxPC3-luc cells were significantly reduced by the pretreatment of excess amount of a PDGFRβ ligand, IQP, or non-radiolabeled compounds, IIQP or IB-IQP (Figure 4).

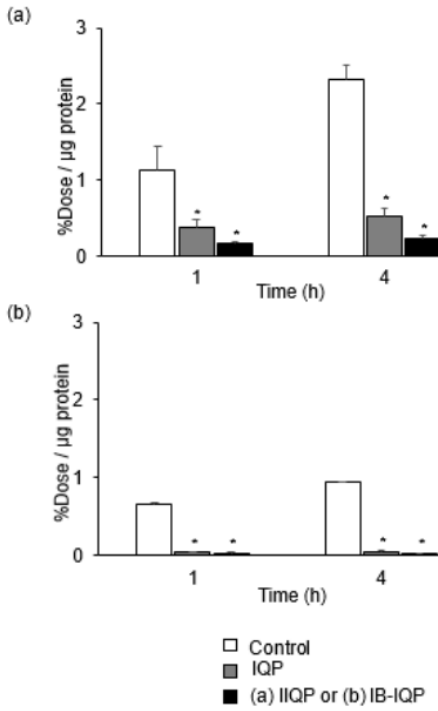

Figure 4. *In vitro* blocking study of (a) [^{125}I]IIQP and (b) [^{125}I]IB-IQP in BxPC3-luc cells. Data were presented as mean ± SD for three samples. Significance was determined using a one-way ANOVA followed by Dunnett's post hoc test ($^{*}p < 0.001$, vs control [^{125}I]IIQP or [^{125}I]IB-IQP).

2.7. Competitive binding assay using BxPC3-luc cells

The competitive binding of [^{125}I]IIQP to BxPC3-luc cells was investigated in the presence of PDGFRβ ligand, IQP, IIQP, and IB-IQP. The IC_{50} values were found to be 311 ± 82 nM for IQP, 44 ± 17 nM for IIQP, and 422 ± 54 nM for IB-IQP.

2.8. Biodistribution studies

Biodistribution of [^{125}I]IIQP and [^{125}I]IB-IQP in normal mice is summarized in Table 1. High accumulation of radioactivity after administration in liver, small intestine, and large intestine were shown. It was excreted into feces from these tissues during 24 h. It indicated that main excretion route of both [^{125}I]IIQP and [^{125}I]IB-IQP was hepatobiliary. It was confirmed that the radioactivity in feces excreted during 24 h after injection of [^{125}I]IIQP and [^{125}I]IB-IQP (75.93 and 68.75 %ID, respectively) were much higher than the radioactivity in urine (3.79 and 13.48 %ID, respectively).

Additionally, radioactivity was hardly observed in any tissues after 24 h evaluation for both radiotracers.

Table 1. Biodistribution of [^{125}I]IIQP and [^{125}I]IB-IQP at 2, 10 min, 1, 4, and 24 h after i.v. injection in ddY mice.

Tissues	Time after injection				
	2 min	10 min	1 h	4 h	24 h
[^{125}I]IIQP					
Blood	3.54 (0.21)	1.05 (0.15)	0.32 (0.03)	0.11 (0.01)	0.02 (0.02)
Liver	13.28 (1.16)	10.29 (0.86)	3.60 (0.59)	1.49 (0.42)	0.25 (0.04)
Kidney	14.85 (0.28)	15.09 (1.41)	9.54 (1.40)	3.55 (0.93)	0.16 (0.04)
Small intestine	2.91 (0.13)	11.19 (1.40)	28.53 (2.30)	6.89 (1.52)	0.06 (0.01)
Large intestine	0.84 (0.07)	0.75 (0.07)	1.59 (0.33)	52.43 (1.70)	0.17 (0.05)
Spleen	6.78 (0.96)	4.79 (0.49)	1.28 (0.13)	0.28 (0.09)	0.03 (0.00)
Pancreas	5.46 (0.41)	3.81 (0.41)	2.45 (0.24)	1.09 (0.13)	0.03 (0.01)
Lung	23.65 (1.45)	9.81 (1.54)	6.66 (2.29)	2.87 (0.54)	0.09 (0.00)
Heart	10.14 (0.75)	3.98 (0.28)	0.78 (0.11)	0.22 (0.01)	0.03 (0.00)
Stomach†	1.11 (0.16)	1.30 (0.09)	1.45 (0.29)	1.09 (0.20)	0.09 (0.03)
Bone	2.21 (0.29)	1.36 (0.15)	0.73 (0.05)	0.11 (0.00)	0.05 (0.01)
Muscle	3.46 (0.42)	1.96 (0.26)	0.65 (0.12)	0.18 (0.02)	0.01 (0.00)
Brain	0.19 (0.02)	0.06 (0.00)	0.03 (0.00)	0.02 (0.00)	0.00 (0.00)
Urine					3.79 (0.71)
Feces					75.93 (4.13)
[^{125}I]IB-IQP					
Blood	2.18 (0.22)**	1.15 (0.17)	0.29 (0.03)	0.07 (0.01)**	0.02 (0.00)
Liver	21.11 (1.02)**	18.99 (1.32)**	3.93 (0.38)	0.57 (0.06)**	0.07 (0.00)**
Kidney	9.30 (1.15)**	5.67 (0.73)**	1.48 (0.45)**	0.39 (0.06)**	0.04 (0.00)**
Small intestine	2.72 (0.40)	11.55 (3.07)	31.10 (2.25)	0.72 (0.10)**	0.01 (0.00)**
Large intestine	0.75 (0.02)	0.95 (0.04)**	1.20 (0.25)	16.53 (3.01)**	0.07 (0.00)*
Spleen	3.25 (0.47)**	2.09 (0.33)**	0.51 (0.05)**	0.09 (0.01)**	0.01 (0.00)**
Pancreas	3.64 (0.37)**	2.71 (0.54)*	0.94 (0.15)**	0.16 (0.01)**	0.00 (0.00)*
Lung	4.98 (1.83)**	2.02 (0.28)**	1.15 (0.25)**	0.63 (0.05)**	0.03 (0.01)**
Heart	5.95 (0.44)**	1.84 (0.30)**	0.50 (0.04)**	0.09 (0.01)**	0.00 (0.00)**
Stomach†	0.92 (0.03)	2.03 (0.89)	1.65 (0.38)	0.19 (0.09)**	0.01 (0.00)**
Bone	1.52 (0.26)*	0.81 (0.16)**	0.31 (0.04)**	0.06 (0.01)**	0.00 (0.00)**
Muscle	1.89 (0.37)**	1.09 (0.15)**	0.33 (0.01)**	0.08 (0.03)**	0.01 (0.00)
Brain	0.30 (0.06)*	0.20 (0.04)**	0.05 (0.00)*	0.02 (0.00)	0.00 (0.00)
Urine					13.48 (0.43)**
Feces					68.75 (6.44)

Data were presented as %injected dose / gram tissue. Each value represent mean ± SD for three or four mice. Significance was determined using an unpaired Student's *t*-test ($^{*}p < 0.05$, $^{**}p < 0.01$ vs. [^{125}I]IIQP).
† presented as %ID/organ.

Biodistribution of [^{125}I]IIQP and [^{125}I]IB-IQP in BxPC3-luc tumor-bearing mice is summarized in Table 2. Accumulation of radioactivity in tumor at 1 h postinjection of [^{125}I]IIQP (1.29 %ID/gram) was significantly higher than that of [^{125}I]IIB-IQP (0.52 %ID/gram) in biodistribution experiments using BxPC3-luc tumor-bearing mice. Accumulation of radioactivity in tumor at 4 h postinjection of [^{125}I]IIQP was 0.45 %ID/gram, which was lower than that at 1 h postinjection.

Table 2. Biodistribution of [^{125}I]IIQP and [^{125}I]IB-IQP at 1 h and 4 h after i.v. injection in BxPC3-luc tumor-bearing mice.

Tissues	[^{125}I]IIQP		[^{125}I]IB-IQP
	1 h	4 h	1 h
Blood	0.69 (0.10)	0.15 (0.01)	0.23 (0.03)**
Liver	11.10 (2.64)	1.48 (0.10)	4.81 (0.66)*
Kidney	15.60 (2.05)	2.65 (0.37)	1.13 (0.09)**
Small intestine	37.37 (3.11)	3.98 (0.44)	45.53 (2.53)*
Large intestine	3.98 (1.35)	22.09 (2.87)	7.88 (3.74)
Spleen	3.46 (0.45)	0.35 (0.09)	0.61 (0.06)**
Pancreas	7.67 (2.50)	2.20 (0.20)	1.23 (0.16)*
Lung	12.28 (0.94)	2.73 (0.44)	1.16 (0.23)**
Heart	1.37 (0.13)	0.29 (0.07)	0.44 (0.02)**
Stomach†	2.99 (1.09)	0.20 (0.03)	0.26 (0.06)*
Bone	1.37 (0.13)	0.03 (0.05)	0.29 (0.03)**
Muscle	1.14 (0.25)	0.13 (0.01)	0.38 (0.03)**
Brain	0.14 (0.02)	0.03 (0.00)	0.05 (0.00)**
BxPC3-luc tumor	1.29 (0.43)	0.45 (0.04)	0.52 (0.09)*

Data were presented as means ± SD of %injected dose / gram of tissue for three or four mice. Significance was determined using an unpaired Student's *t*-test ($^{*}p < 0.05$, $^{**}p < 0.01$ vs. [^{125}I]IIQP).
† presented as %ID/organ.

In *in vivo* blocking studies, the effect of IQP, a high affinity ligand for PDGFRβ, on tumor uptake of [^{125}I]IIQP at 1 h after administration is shown in Figure 5. In this case, the radioactivity level in the blood after injection of [^{125}I]IIQP was significantly increased by pretreatment of IQP. The values of % injected dose per gram of control group and IQP pretreatment group were 0.69 ± 0.10 and 3.16 ± 0.15, respectively. Thus, the figures are shown as not only % injected dose per gram but also as tumor / blood ratio. The result demonstrated that pretreatment of an excess amount of IQP resulted in a significant decrease in tumor uptake and the uptake ratio of tumor to blood at 1 h postinjection of [^{125}I]IIQP.

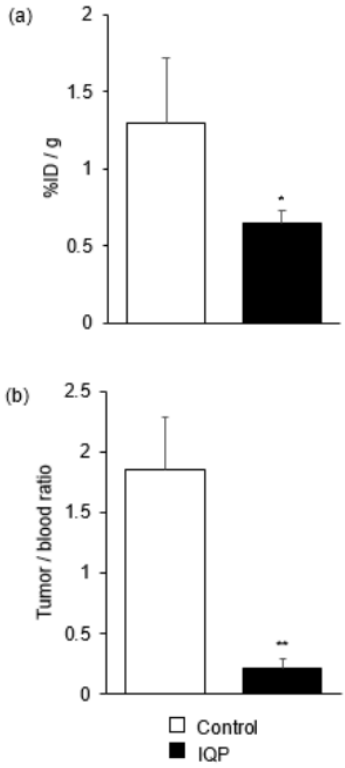

Figure 5. Tumor uptake and tumor/blood uptake ratios of [^{125}I]IIQP at 1 h postinjection with IQP (40 mg/kg) (blocking group) or control group. Data were presented as means ± SD for three or four mice. Significance was determined using an unpaired Student's *t*-test ($^{*}p < 0.05$, $^{**}p < 0.001$).

3. Discussion

To develop probes for PDGFRβ imaging, the affinity of newly synthesized IQP analogs, which contain iodine molecules, for PDGFRβ, was evaluated using WST-8 assay. WST-8 assay determines cell viability; therefore, it cannot directly be used for affinity studies. A negative correlation is speculated between the PDGFRβ-analog affinity and TR-PCT1 cell viability because TR-PCT1 cells express PDGFRβ, and they die when the receptor signaling pathway is interrupted.[41,42] Therefore, WST-8 assay was used as an index to evaluate affinity changes between the ligand and PDGFRβ by introducing an iodine molecule in IQP. IB-IQP and IQP displayed similar affinity for PDGFRβ as a molecular target, whereas IIQP displayed a higher affinity than that of IQP (Figure 2). A competitive binding assay was also performed to evaluate the affinity of ligands for PDGFRβ. The competitive binding of [^{125}I]IIQP to BxPC3-luc cells was investigated in the presence of PDGFRβ ligands, IQP, IIQP, and IB-IQP. In this assay, [^{125}I]IIQP do not always bind to only PDGFRβ in tumor cells. Thus, the IC_{50} values of the experiments may not indicate the affinity for PDGFRβ completely. However, the IC_{50} values should be an index of the affinity. As the results, the IC_{50} value of IIQP (44 nM) was lower than those of IQP (311 nM) and IB-IQP (422 nM), indicating that IIQP possesses higher affinity than IQP and IB-IQP. It was consistent with WST-8 assay. Generally, the introduction of certain molecules, functional groups or elements into lead compounds can reduce their affinity for target molecules. However, in this study, the introduction of iodine into IQP increased the affinity of IIQP for PDGFRβ. This result is extremely favorable for developing molecular probes for PDGFRβ imaging.

Iodogen, chloramine-T (CAT), NCS, and peracetic acid (PAA) are commonly used as oxidizing agents for the preparation of radioiodinated compounds. [^{125}I]IIQP and [^{125}I]IB-IQP were synthesized using an iododestannylation technique without the addition of a carrier and using NCS as an oxidizing agent with excellent radiochemical yields. We also tried to synthesize [^{125}I]IIQP and [^{125}I]IB-IQP using CAT and PAA as oxidizing agents; however, the radiochemical yields were <50%. These results indicated that NCS is the most suitable oxidizing agent for compounds with oligo arene, such as IIQP and IB-IQP.

In cellular uptake experiments for [^{125}I]IIQP and [^{125}I]IB-IQP, these radiotracers showed higher accumulation in PDGFRβ-positive tumor cells (BxPC3-luc) than in PDGFRβ-negative tumor cells (MCF7). [^{125}I]IIQP, which had the highest affinity for PDGFRβ in the competitive binding assay and WST-8 assay, showed higher accumulation in PDGFRβ-positive tumor cells than that of [^{125}I]IB-IQP (Figure 3). In *in vivo* experiments, [^{125}I]IIQP showed significantly higher accumulation in BxPC3-luc tumor than that of [^{125}I]IB-IQP (Table 2). Moreover, the uptake of [^{125}I]IIQP in PDGFRβ-positive tumor cells was inhibited by treatment with an excess amount of PDGFRβ ligand both in the cellular uptake study (Figure 4) and in the *in vivo* blocking experiments using tumor-

bearing mice (Figure 5). These results indicated that the uptake of [^{125}I]IIQP in tumors is PDGFRβ-specific, and it must bind the ATP-binding site of PDGFRβ in the tumor cell.

Small molecule TKIs, including [^{125}I]IIQP and [^{125}I]IB-IQP, target the intracellular domain of RTKs, and for this binding, they should diffuse through the cellular membrane. The log *P* values of the compounds are an important factor to penetrate the cellular membrane. It has been shown that a log *P* value of 1 to 3.5 is required to passively penetrate cellular membrane.[43-46] In this study, Log *P* values of [^{125}I]IIQP and [^{125}I]IB-IQP were 2.71 and 3.19, respectively. This suggested that the lipophilicity of both the radiotracers was suitable for them to be used as PDGFRβ imaging probes.

In the biodistribution experiments, [^{125}I]IIQP and [^{125}I]IB-IQP were mainly excreted through the hepatobiliary pathway, which is often observed for small molecule radiotracers directed to the ATP-binding site of TKs.[20,23,47,48] This excretion route may be due to the moderately high lipophilicities of these radiotracers. Meanwhile, it has been known that free iodine accumulates in the stomach and thyroid; this is used as an index of deiodination of radioiodine-labeled tracers *in vivo*. In this study, the accumulation in the stomach was not high, suggesting that both [^{125}I]IIQP and [^{125}I]IB-IQP are highly stable not only *in vitro* but also *in vivo*. In the case of [^{125}I]IIQP, the biodistribution study in tumor-bearing mice at 4 h postinjection was performed because we expected more effective tumor detection derived from higher accumulation ratios of tumor / non-target tissues. The results showed that the tumor accumulation decreased; however, tumor to blood and tumor to muscle ratios at 4 h postinjection were higher than those at 1 h postinjection because radioactivity in the blood and muscle was prominently decreased. Many studies have reported that P glycoprotein (P-gp), breast cancer resistant protein (BCRP), and/or other drug efflux transporters can hinder tumor uptake of anticancer drugs.[49,50] Planar structure, high lipophilicity, and neutral or positive charges are some of requirements for P-gp substrates.[51] Because [^{125}I]IIQP possesses these characteristics, it can be a substrate for P-gp and therefore, its accumulation may have decreased in tumor cells. However, further research is warranted to prove whether [^{125}I]IIQP is a P-gp substrate. Another possibility is the presence of radioactive metabolites that have less or no affinity to the molecular target. Rapid metabolism leads to the loss of affinity for target molecules and resulting low tumor uptake.[52] Although [^{125}I]IIQP showed high stability both *in vitro* and *in vivo*, this possibility cannot be completely excluded because we did not perform a metabolic study.

4. Conclusion

In this study, we synthesized the radiolabeled compounds [^{125}I]IIQP and [^{125}I]IB-IQP using an iododestannylation reaction under non-carrier added condition with high radiochemical yields and high purities. This method can also be used to synthesize other radioiodinated compounds containing quinoline-benzimidazole derivatives. The present study showed that radioiodinated IIQP could be a promising imaging agent compared with radioiodinated IB-IQP. However, modification of its structure may be needed to obtain appropriate PDGFRβ-targeted imaging agents, which have higher tumor uptake and tumor to background ratios.

References

1. Yu, J.; Ustach, C.; Kim, H. R. C. J. Biochem Mol Biol. 2003, 36, 49-59.
2. Criscitiello, C.; Gelao, L.; Viale, G.; Esposito, A.; Curigliano, G. Expert Opin Investig Drugs. 2014, 23, 599-610.
3. Östman, A.; Heldin, C. H. Adv Cancer Res 2007, 97, 247-274
4. Levitzki, A.; Gazit, A. Science. 1995, 267, 1782-1788.
5. Östman, A. Cytokine Growth Factor Rev. 2004, 15, 275-286.
6. Lindborg, M.; Cortez, E.; Höidén-Guthenberg, I.; Gunneriusson, E.; von Hage, E.; Syud, F.; Morrison, M.; Abrahmsén, L.; Herne, N.; Pietras, K.; Frejd, F. Y. J Mol Biol. 2011, 407, 298-315.
7. Pietras, K.; Sjöblom, T.; Rubin, K.; Heldin, C. H.; Östman, A. Cancer Cell. 2003, 3, 439-443.
8. Benezra, M.; Hambardzumyan, D.; Penate-Medina, O.; Veach, D. R.; Pillarsetty, N.; Smith-Jones, P.; Phillips, E.; Ozawa, T.; Zanzonico, P. B.; Longo, V.; Holland, E. C.; Larson, S. M.; Bradbury, M. S. Neoplasia. 2012, 14, 1132-1143.
9. Cornelissen, B. J Labelled Comp Radiopharm. 2014, 57, 310-316.
10. Fass, L. Mol Oncol. 2008, 2, 115-152
11. Cunha, L.; Szigeti, K.; Mathé, D.; Metello, L. F. Drug Discov Today. 2014, 19, 936-948.
12. Poot, A. J.; Slobbe, P.; Hendrikse, N. H.; Windhorst, A. D.; van Dongen, G. A. Clin Pharmacol Ther. 2013, 93, 239-241.
13. Fretto, L. J.; Snape, A. J.; Tomlinson, J. E.; Seroogy, J. J.; Wolf, D. L.; LaRochelle, W. J.; Giese, N. A. J Biol Chem. 1993, 268, 3625-3631.
14. Maudsley, S.; Zamah, A. M.; Rahman, N.; Blitzer, J. T.; Luttrell, L. M.; Lefkowitz, R. J.; Hall, R. A. Mol Cell Biol. 2000, 20, 8352-8363.
15. Camorani, S.; Esposito, C. L.; Rienzo, A.; Catuogno, S.; Iaboni, M,; Condorelli, G.; de Franciscis, V.; Cerchia, L. Mol Ther. 2014, 22, 828-841.
16. Tolmachev, V.; Varasteh, Z.; Honarvar, H.; Hosseinimehr, S. J.; Eriksson, O.; Jonasson, P.; Frejd, F. Y.; Abrahmsen, L.; Orlova, A. J Nucl Med. 2014, 55, 294-300.
17. Strand, J.; Varasteh, Z.; Eriksson, O.; Abrahmsen, L.; Orlova, A.; Tolmachev, V. Mol Pharm. 2014, 11, 3957-3964.
18. Askoxylakis, V.; Marr, A.; Altmann, A.; Markert, A.; Mier, W.; Debus, J.; Huber, P. E.; Haberkorn, U. Mol Imaging Biol. 2013, 15, 212-221.
19. Marr, A.; Nissen, F.; Maisch, D.; Altmann, A.; Rana, S.; Debus, J.; Huber, P. E.; Haberkorn, U.; Askoxylakis, V. Mol Imaging Biol. 2013, 15, 391-400.
20. Yoshimoto, M.; Hirata, M.; Kanai, Y.; Naka, S.; Nishii, R.; Kagawa, S.; Kawai, K.; Ohmomo, Y. Biol Pharm Bull. 2014, 37, 355-360.
21. Yeh, H. H.; Ogawa, K.; Balatoni, J.; Mukhapadhyay, U.; Pal, A.; Gonzalez-Lepera, C.; Shavrin, A.; Soghomonyan, S.; Flores, L. II.; Young, D.; Volgin, A. Y.; Najjar, A. M.; Krasnykh, V.; Tong, W.; Alauddin, M. M.; Gelovani, J. G. Proc Natl Acad Sci U S A. 2011, 108, 1603-1608.

22. Fernandes, C.; Oliveira, C.; Gano, L.; Bourkoula, A.; Pirmettis, I.; Santos, I. Bioorg Med Chem. 2007, 15, 3974-3980.
23. Hirata, M.; Kanai, Y.; Naka, S.; Yoshimoto, M.; Kagawa, S.; Matsumuro, K.; Katsuma, H.; Yamaguchi, H.; Magata, Y.; Ohmomo, Y. Ann Nucl Med. 2013, 27, 431-443.
24. Kuchar, M.; Oliveira, M. C.; Gano, L.; Santos, I.; Kniess, T. Bioorg Med Chem Lett. 2012, 22, 2850-2855.
25. Wang, J. Q.; Miller, K. D.; Sledge, G. W.; Zheng, Q. H. Bioorg Med Chem Lett. 2005, 15, 4380-4384.
26. Wang, J. Q.; Gao, M.; Miller, K. D.; Sledge, G. W.; Zheng, Q. H. Bioorg Med Chem Lett. 2006, 16, 4102-4106.
27. Galbán, C. J.; Galbán, S.; Van Dort, M. E.; Luker, G. D.; Bhojani, M. S.; Rehemtulla, A.; Ross, B. D. Prog Mol Biol Transl Sci. 2010, 95, 237-398.
28. Tolmachev, V.; Stone-Elander, S.; Orlova, A. Lancet Oncol. 2010, 11, 992-1000.
29. Roberts, W. G.; Whalen, P. M.; Soderstrom, E.; Moraski, G.; Lyssikatos, J. P.; Wang, H. F.; Cooper, B.; Baker, D. A.; Savage, D.; Dalvie, D.; Atherton, J. A.; Ralston, S.; Szewc, R.; Kath, J. C.; Lin, J.; Soderstrom, C.; Tkalcevic, G.; Cohen, B. D.; Pollack, V.; Barth, W.; Hungerford, W.; Ung, E. Cancer Res. 2005, 65, 957-966.
30. Xi, Y.; Chen, M.; Liu, X.; Lu, Z.; Ding, Y.; Li, D. Onco Targets Ther. 2014, 7, 1215-1221.
31. Asashima, T.; Iizasa, H.; Terasaki, T.; Hosoya, K.; Tetsuka, K.; Ueda, M.; Obinata, M.; Nakashima, E. Eur J Cell Biol. 2002, 81, 145-152.
32. Weichert, D.; Banerjee, A.; Hiller, C.; Kling, R. C.; Hübner, H.;, Gmeiner, P. J Med Chem. 2015, 58, 2703-2717.
33. Sundriyal, S.; Malmquist, N. A.; Caron, J.; Blundell, S.; Liu, F.; Chen, X.; Srimongkolpithak, N.; Jin, J.; Charman, S. A.; Scherf, A.; Fuchter, M. J. ChemMedChem. 2014, 9, 2360-2373.
34. Zalutsky, M. R.; Narula, A. S. Int J Rad Appl Instrum A. 1987, 38, 1051-1055.
35. Arano, Y.; Wakisaka, K.; Ohmomo, Y.; Uezono, T.; Mukai, T.; Motonari, H.; Shiono, H.; Sakahara, H.; Konishi, J.; Tanaka, C.; Yokoyama, A. J Med Chem. 1994, 37, 2609-2618.
36. Barth, W.; Luzzio, M.; Lyssikatos, J. European Patent EP 1 235 825 B1, 2006, 1-136.
37. Niihama, K. Jpn. Kokai Tokkyo Koho Patent JP 2008031067, 2008.
38. Ogawa, K., Shiba, K.; Akhter, N.; Yoshimoto, M.; Washiyama, K.; Kinuya, S.; Kawai, K.; Mori, H. Cancer Sci. 2009, 100, 2188-2192.
39. Ogawa, K.; Kanbara, H.; Kiyono, Y.; Kitamura, Y.; Kiwada, T.; Kozaka, T.; Kitamura, M.; Mori, T.; Shiba, K.; Odani, A. Nucl Med Biol. 2013, 40, 445-450.
40. Chung, H.W.; Wen, J.; Lim, J. B.; Bang, S.; Park, S. W.; Song, S. Y. Int J Radiat Oncol Biol Phys. 2009. 75, 862-869.
41. Riese, D. J. Expert Opin Drug Discov. 2011, 6, 185-193
42. Weisberg, E.; Manley, P.; Mestan, J.; Cowan-Jacob, S.; Ray, A.; Griffin, J. D. Br J Cancer. 2006, 94, 1765-1769.
43. Waterhouse, R. N. Mol Imaging Biol. 2003, 5, 376-389.
44. Pike, V. W. Trends Pharmacol Sci. 2009, 30, 431-440.

45. Dishino, D.D.; Welch, M. J.; Kilbourn, M. R.; Raichle, M. E. J Nucl Med. 1983, 24, 1030-1038.
46. VanBrocklin, H. F.; Lim, J. K.; Coffing, S. L.; Hom, D. L.; Negash, K.; Ono, M. Y.; Gilmore, J. L.; Bryant, I.; Riese, D. J. II. J Med Chem. 2005, 48, 7445-7456.
47. Zhang, M. R.; Kumata, K.; Hatori, A.; Takai, N.; Toyohara, J.; Yamasaki, T.; Yanamoto, K.; Yui, J.; Kawamura, K.; Koike, S.; Ando, K.; Suzuki, K. Mol Imaging Biol. 2010, 12, 181-191.
48. Samén, E.; Arnberg, F.; Lu, L.; Olofsson, M. H.; Tegnebratt, T.; Thorell, J. O.; Holmin, S.; Stone-Elander, S. J Nucl Med. 2013, 54, 1804-1811.
49. Asakawa, C.; Ogawa, M.; Kumata, K.; Fujinaga, M.; Kato, K.; Yamasaki, T.; Yui, J.; Kawamura, K.; Hatori, A.; Fukumura, T.; Zhang, M. R. Bioorg Med Chem Lett. 2011, 21, 2220-2223.
50. Chen, Y.; Agarwal, S.; Shaik, N. M.; Chen, C.; Yang, Z.; Elmquist, W. F. J Pharmacol Exp Ther. 2009, 330, 956-963.
51. Ogushi, N.; Sasaki, K.; Shimoda, M. J Vet Med Sci. 2017, 79, 320-327.
52. Slobbe, P.; Poot, A. J.; Haumann, R.; Schuit, R. C.; Windhorst, A. D.: van Dongen, G. A. Nucl Med Biol. 2016, 43, 612-624.

[125I]IIQP for PDGFRb imaging

ORIGINALITY REPORT

12%	6%	11%	1%
SIMILARITY INDEX	INTERNET SOURCES	PUBLICATIONS	STUDENT PAPERS

PRIMARY SOURCES

1	Kazuma Ogawa, Hiroya Kanbara, Yasushi Kiyono, Yoji Kitamura et al. "Development and evaluation of a radiobromine-labeled sigma ligand for tumor imaging", Nuclear Medicine and Biology, 2013 Publication	2%
2	Kazuma Ogawa, Hiroaki Echigo, Kenji Mishiro, Saki Hirata et al. " Ga- and At-Labeled RGD Peptides for Radiotheranostics with Multiradionuclides ", Molecular Pharmaceutics, 2021 Publication	2%
3	www.labome.org Internet Source	2%
4	preview-ejnmmires.springeropen.com Internet Source	1%
5	Weijun Wei, Zachary T. Rosenkrans, Jianjun Liu, Gang Huang, Quan-Yong Luo, Weibo Cai. "ImmunoPET: Concept, Design, and Applications", Chemical Reviews, 2020 Publication	1%

6	Julie Bolcaen, Shankari Nair, Cathryn H. S. Driver, Tebatso M. G. Boshomane, Thomas Ebenhan, Charlot Vandevoorde. "Novel Receptor Tyrosine Kinase Pathway Inhibitors for Targeted Radionuclide Therapy of Glioblastoma", Pharmaceuticals, 2021 Publication	1 %
7	Kazuma Ogawa, Takuya Takeda, Masaru Yokokawa, Jing Yu, Akira Makino, Yasushi Kiyono, Kazuhiro Shiba, Seigo Kinuya, Akira Odani. "Comparison of Radioiodine- or Radiobromine-Labeled RGD Peptides between Direct and Indirect Labeling Methods", Chemical and Pharmaceutical Bulletin, 2018 Publication	1 %
8	devbio.jbc.org Internet Source	1 %
9	Kazuma Ogawa, Jing Yu, Atsushi Ishizaki, Masaru Yokokawa, Masanori Kitamura, Yoji Kitamura, Kazuhiro Shiba, Akira Odani. "Radiogallium Complex-Conjugated Bifunctional Peptides for Detecting Primary Cancer and Bone Metastases Simultaneously", Bioconjugate Chemistry, 2015 Publication	1 %
10	eprints.gla.ac.uk Internet Source	1 %

Exclude quotes	Off	Exclude matches	< 1%
Exclude bibliography	On		